Dielectric Spectroscopy of a Nanofiltration Membranes−Electrolyte Solution System: I. Low-Frequency Dielectric Relaxation from the Counterion Polarization in Pores and Model Development

Qing Lu and Kongshuang Zhao*

College of Chemistry, Beijing Normal University, Beijing 100875

Received: October 23, 2010

The dielectric spectra of nanofiltration membranes NF90, NF-, and NF270 in eight electrolytes, NaCl, KCl, $CuCl_2$, $MgCl_2$, Na_2SO_4, K_2SO_4, $MgSO_4$, and $CuSO_4$, were investigated as a function of the electrolyte concentration over a frequency range from 40 Hz to 11 MHz. Two relaxations were observed: the one at high frequency was caused by interfacial polarization between the membrane and electrolyte, and the low-frequency relaxation, on which we focus on in this work, was confirmed to be due to the counterion polarization effects in the pores of the membrane. A model of cylindrical pores which were dispersed in membrane base was developed to interpret the low-frequency relaxation. On the basis of this model, we amended the expression deduced by Takashima for describing the dielectric behavior of a cylinder particle suspension to fit our dielectric data from the low-frequency relaxation. The data fitting with this improved expression was suitable for all the systems measured in this work; structural and electrical parameters such as the radius of the pore in the membrane, the thickness of the active layer of the membrane, surface charged density, and zeta potential on the pore wall were obtained finally.

1. Introduction

Nanofiltration (NF) membranes are kinds of typical charged weakly and porous separation membranes with nanoscale in general. Even though applications of NF membranes have expanded rapidly during the last decades,[1] the transport mechanism of the ion in NF membranes has not been fully understood yet. In the study of their performance, they are usually viewed as a bundle of capillaries with effective structural features, such as pore size, membrane thickness, and porosity. Those features affect the mass transporting of the membrane, for instance, a pore diameter of around a few nanometers results in steric hindrance, which plays a role in the separation of solutes, and the thickness and porosity of the membrane will influence the permeate flux in the transport process. On the other hand, since the ion separation resulting from the electrostatic interactions between ions and membrane is based on the fixed charge of the membrane, the electrical properties of NF membrane are another important aspect in the transporting process of the salts. Additionally, the charge density and zeta potential on the pore wall can also imply that solute exclusion results from a complex mechanism involving several phenomena.[2,3] From this, accurate calculation of the structural and electrical parameters of NF membranes from the experimental data is one of the key problems in the study on the separation process of NF membranes.

Several methods are used to study the structural and electrical properties of NF membranes, such as measuring the membrane potential, streaming potential, and measuring salt permeability.[4−7] Dielectric spectroscopy, which is the same experimental method as impedance measurement but different in the way of data conversion and analyzing, is also an important method to study membrane/solution systems in which more than one interface exists. Dielectric spectroscopy, as a noninvasive method and being especially sensitive to the heterogeneous system,[8] has been successfully applied in the study on membrane systems by a few research groups, including the authors' group.[9−19] H. G. L. Coster and co-workers studied various reparation membranes; for instance, they determined the stability of the supporting liquid membrane,[9] characterized the electrical properties and porosity of ultrafiltration membranes,[10] and discussed fouling of reverse osmosis membranes by analyzing the electrical and structural parameters;[11] Juana Benavente et al. characterized the supported ionic liquid membranes and assessed the impact of the presence of water on the electrical properties of the membranes;[12] E. K. Zholkovskij proposed a theory of low-frequency impedance in membranes consisting of several layers and used irreversible thermodynamics to calculate the frequency characteristics of the system;[13] Jin-Soo Park et al. investigated ion-exchange membrane systems using impedance spectroscopy, suggested an equivalent circuit to quantitatively analyze each component of the system, and obtained the resistance and capacitance of the membrane;[14] Monika Naumowicz et al. studied two-component lipid membranes by electrochemical impedance spectroscopy and determined parameters of the complex including capacitance, conductance, and area occupied by the complex molecule;[15] Michael J. Kelly et al. evaluated the local conductivity of Nafion membranes by the use of electrochemical impedance spectroscopy with microelectrodes and found that small amounts of contaminants can have a detrimental effect on the conductivity in the membrane.[16] In our previous study of nanofiltration membrane/electrolyte systems, we found two relaxations: the one at high frequency was due to the interfacial polarization (Maxwell−Wagner effect), and the one at low frequency was considered to be due to the little ununiformity of the membrane structure. By analyzing the dielectric spectra on the base of the model, information on the distribution of the ion conductivity in

* To whom correspondence should be addressed. Phone: +86010-58808283. E-mail: zhaoks@bnu.edu.cn.

10.1021/jp110160z © 2010 American Chemical Society
Published on Web 11/23/2010

different layers of the membrane was obtained.[18] However, in these studies, membranes were always investigated as an integrated whole, little research was concerned about the inner dielectric properties of the membrane, and properties of the pores in the membrane have not been reported.

The low-frequency relaxation, named α-relaxation generally, is assigned to be caused by counterion polarization in biological and colloid suspension fields.[20,21] Nevertheless, in the study on the membrane/solution system, the low-frequency relaxation was assumed to arise from counterion relaxation effects in the pores of the membrane.[22,23] Wensheng Kuang carried out dielectric measurements on thin plastic membranes with different thickness, pore size, and pores numbers and discussed the low-frequency relaxation.[22] Ørjan G. Martinsen studied dielectric relaxation of microporous membranes in electrolyte, assumed the low-frequency relaxation to be caused by counterion relaxation effects in the pores, and provided a rough estimate on measurements by Schwarz theory.[23] Moreover, the reason for the low-frequency dielectric behavior of the membrane/electrolyte system has not been thoroughly clarified yet, and the electrical and structural information involved in it has not been discussed in detail.

In the present work, dielectric measurements for a series of membrane/electrolyte solution systems have been measured in the frequency range from 40 Hz to 11 MHz by varying the concentration of the electrolyte. The systems were made up as follows: three types of NF membrane (NF90, NF270, NF-) immersed in eight kinds of electrolyte solutions at various concentrations. Two relaxation processes were observed at around 10^2 and 10^5 Hz. Detailed analysis for the dielectric spectra were focused on the low-frequency relaxation to obtain the interior properties of the constituent phases, especially the membrane and the pore inside the membrane. The analytical method combined with the Cole−Cole experiential function was employed to investigate the relaxation mechanism of the low-frequency spectra. Simultaneously, in order to gain more inner information on the membrane, a pore−membrane base dispersion model was developed and the expression deduced by Takashima for describing the dielectric behavior of a cylinder particle suspension was amended.[24] We showed that the parameters related to the structural and electrical properties inside the membrane can be well estimated by using the developed model and the improved expression.

2. Experimental and Methods

2.1. Nanofiltration Membranes. The three types of commercial NF membranes used in this study were NF90, NF-, and NF270, which were purchased from Filmtec (Dow, USA). These membranes have a typical double-layer structure. The two layers in the membrane are composed of a thin polyamide film as the active layer and a large mesoporous polysulfone as the support layer. The membranes are negatively charged in solution by partial dissociation of the carboxyl groups (−COOH). The support layer of the membranes was peeled off, and the remaining part of the membrane was the active layer with a thickness of 0.2 μm.

2.2. Dielectric Measurements. The measuring cell made of methacrylate resin consists of a pair of platinum disk electrodes whose area S is 3.14 cm^2. A specimen membrane separated the cylindrical compartments between the electrodes, and the two compartments were filled with aqueous solutions of the same electrolyte and identical concentration. In other words, the nanofiltration membrane used in this work was sandwiched between two aqueous solution phases to form a solution/membrane/solution system. The membrane area effective for dielectric measurement was made equal to that of the electrodes. The cell constant S/L was measured to be 2.6 cm, and L is the distance between the two electrodes. A figure of the measuring cell is in the literature.[25]

The active layer of the membrane was rinsed with enough deionized water to remove organic impurities and salt in the membrane. Before dielectric measurements, the membrane (hereafter, the term membrane refers to the active layer of membrane) was immersed in deionized water for 24 h to remove air in the membrane and then in the most dilute solution of $MgCl_2$ for more than 3 h in order to equilibrate the ions in the solution and the membrane. The capacitance C and conductance G of the membrane in $MgCl_2$ solutions of increasing concentration were measured with an Agilent 4294A Precision Impedance Analyzer, operating over the frequency range from 40 Hz to 11 MHz, under an applied ac voltage of 0.05 V. The measuring cell was placed still for 15 min when the solutions were changed to higher concentration one at a time. Dielectric measurements were also carried out for the same membranes in solutions of seven other electrolytes, NaCl, KCl, $CuCl_2$, Na_2SO_4, K_2SO_4, $MgSO_4$, and $CuSO_4$, with the same method. The concentrations of these electrolytes were from 0.05 to 7 mol·m^{-3}. All measurements were performed between 21 and 22 °C, and all experimental data were subjected to certain corrections for the errors arising from residual inductance due to the cell assembly.[26] The permittivity, ε, and conductivity, κ, were calculated from the corrected capacitance and conductance on the basis of eqs 1−4

$$C_S = \frac{C_x(1 + \omega^2 L_r C_x) + L_r G_x^2}{(1 + \omega^2 L_r C_x)^2 + (\omega L_r G_x)^2} - C_r \quad (1)$$

$$G_S = \frac{G_x}{(1 + \omega^2 L_r C_x)^2 + (\omega L_r G_x)^2} \quad (2)$$

$$\varepsilon = (C_s - C_r)/C_l \quad (3)$$

$$\kappa = G_s \varepsilon_0 / C_l \quad (4)$$

where C_x, G_x, C_s, and G_s are the measured and corrected capacitance and conductance, respectively, ω (=2πf) is the angular frequency, and ε_0 (=8.8541 × 10^{-12} F·m^{-1}) is the permittivity of the vacuum.

3. Results and Discussions

3.1. Dielectric Behavior of the Membrane/Electrolyte Solutions System. All systems composed of the membrane and electrolyte solutions described in section 2.2 were subjected to dielectric measurements over a frequency range from 40 Hz to 11 MHz. Figure 1 shows three-dimensional representations for the concentration dependence of the dielectric spectra of the system composed of NF90 membrane and $MgCl_2$ aqueous solution in the concentration range of 0.05−7 mol·m^{-3}. It is clear from this figure that there are two relaxations appearing and changing among the whole electrolyte concentrations as illustrated by the arrows in Figure 1.

It is obvious from Figure 1a that for relaxation at high frequency, when the concentration of the electrolyte $MgCl_2$ increases, the dielectric relaxation shifts to the higher frequency side, the values of ε for the high-frequency relaxation remain

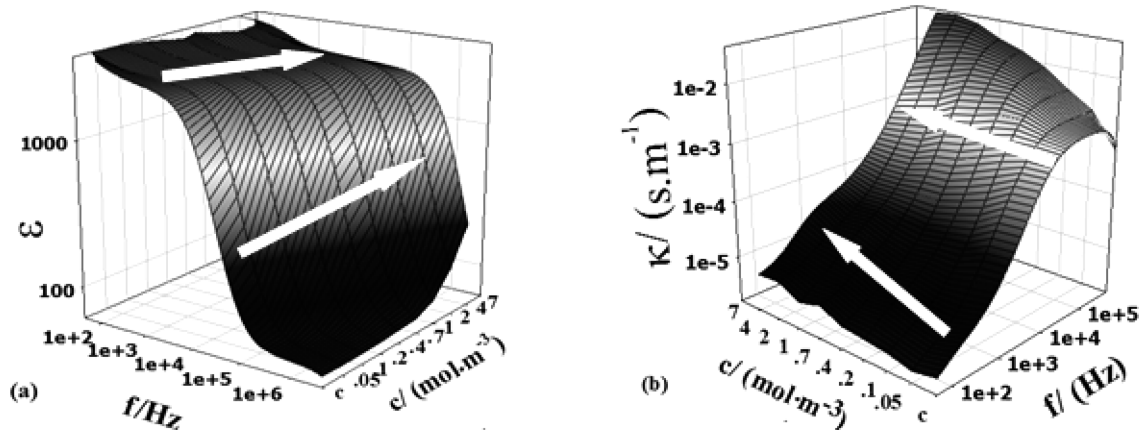

Figure 1. Three-dimensional representations of concentration dependence of (a) the relative permittivity spectrum and (b) the conductivity spectrum for the system composed of the NF90 membrane and the compartments filled with $MgCl_2$ aqueous solution of various concentrations.

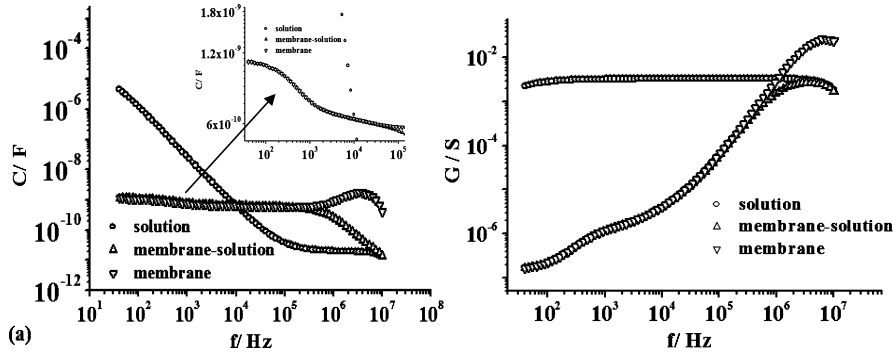

Figure 2. Dielectric spectra ((a) for capacitance, (b) for conductance) of (○) 7.0 mol·m^{-3} $MgCl_2$ solution, (△) membrane−7.0 mol·m^{-3} $MgCl_2$ solution system (obtained from experiment), (▽) only membrane (obtained by subtracting the dielectric response of the solution from the response of the membrane−solution system using the same method used in ref 28).

almost unchanged. This is a typical feature of the M−W interfacial polarization mechanism.[27] The low-frequency relaxation around ca. 10^2 Hz is an alpha relaxation, and it was always assumed to arise from counterion polarization effects in the pores of the membrane.[22,23] Dielectric measurement of conductive materials is difficult at low frequencies, where dielectric relaxation due to counterion polarization appears, because of interference from electrode polarization. In general, for membrane−solution systems, the dielectric response of the membrane could be obtained by subtracting the contribution of the solution from the spectrum of the whole membrane−solution system.[18,28] This method could be used to verify the influence of electrode polarization on the low-frequency relaxation. Therefore, this method was adopted in processing dielectric data of low frequency in this work, and results for one sample (note that a sample with the highest electrolyte concentration was used, of which electrode polarization is the most remarkable) are shown in Figure 2. It can be easily seen from Figure 2 that the dielectric response of the membrane and the response of the membrane−solution system coincide with each other completely at the frequency range below 10^4 Hz. This means the electrode polarization has little impact on the low-frequency relaxation, which was actually caused by the membrane itself in the present work.

To verify the origin of the low-frequency relaxation, a typical one in the low-frequency relaxation range of Figure 1 at a concentration of 1.0 mol·m^{-3} was cut and is shown in Figure 3, where the ε_l, ε_h, κ_l, κ_h (the limiting values of ε and κ at high (subscript h) and low (subscript l) frequencies for the low-frequency relaxation), and f_0 (the character frequency of the low-frequency relaxation, $f_0 = 1/2\pi\tau$, where τ is the relaxation time)

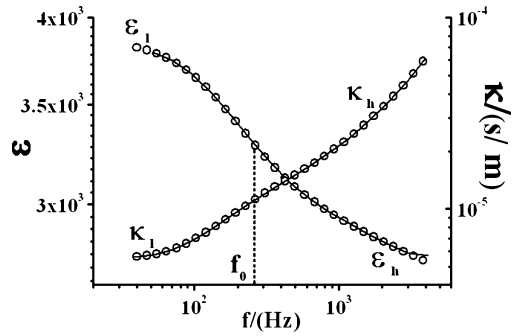

Figure 3. Typical dielectric spectra extracted from Figure 1 at a concentration of 1.0 mol·m^{-3}. The solid lines are the best-fit curves calculated from eq 5.

are used to characterize the low-frequency relaxation. These five parameters are named the dielectric parameter and are generally useful in describing this kind of relaxation.

3.2. Estimation of the Low-Frequency Relaxation Mechanism. ***3.2.1. Determination of Relaxation Parameters from Dielectric Spectra.*** To probe into the origin for the low-frequency relaxation, it is necessary to obtain the dielectric parameters characterizing the relaxation. Therefore, we fitted the dielectric spectra $\varepsilon-f$ curve shown in Figure 3 with the Cole−Cole equation[11]

$$\varepsilon(f) = \varepsilon_h + \frac{(\varepsilon_l - \varepsilon_h)\left[1 + \left(\frac{f}{f_0}\right)^{\beta}\cos\left(\frac{\pi}{2}\beta\right)\right]}{1 + 2\left(\frac{f}{f_0}\right)^{\beta}\cos\left(\frac{\pi}{2}\beta\right) + \left(\frac{f}{f_0}\right)^{2\beta}} \quad (5)$$

TABLE 1: Dielectric Parameters Obtained from Figure 2 and Eqs 5 and 6

concentration (mol·m^{-3})	ε_l	ε_h	$\Delta\varepsilon$	κ_l (μs·m^{-1})	κ_h (μs·m^{-1})	$\Delta\kappa$ (μs·m^{-1})	f_0 (Hz)	τ (ms)	β
0.05	3628	2565	1063	1.864	18.46	16.60	102.8	1.549	1
0.1	3639	2554	1085	1.372	18.07	16.70	120.3	1.324	0.95
0.2	3641	2548	1093	1.924	28.95	27.03	120.3	1.325	0.85
0.4	3720	2551	1169	2.242	65.31	63.07	140.8	1.131	0.84
0.7	3731	2542	1189	2.910	67.30	64.41	164.8	0.966	0.84
1.0	3804	2548	1256	2.634	90.01	84.37	192.9	0.825	0.85
2.0	3988	2556	1432	3.659	160.2	156.6	264.2	0.603	0.86
4.0	4323	2566	1756	6.921	295.8	288.9	390.9	0.407	0.85
7.0	5009	2558	2451	6.447	457.3	450.8	495.8	0.321	0.84

where the meaning of ε_l and ε_h are the same as that described in section 3.1 (see Figure 2), f is the measured frequency, and β is the distribution coefficient of the relaxation time ($0 < \beta \leq 1$), which reflects the complexity of the system's inner structure.[11] The solid lines in Figure 3 are the best-fit curves calculated from eq 5 for the system composed of NF90 membrane and 1.0 mol·m^{-3} $MgCl_2$ electrolyte solution. Because both values of the limiting conductivity of low frequency, κ_h and κ_l, cannot be determined by fitting the data with eq 5, the value of κ_l was determined directly from the curve of $\kappa-f$ in Figure 3 and the value of κ_h was calculated with the following equation[29]

$$\kappa_h = ((\varepsilon_l - \varepsilon_h)2\pi f_0 \varepsilon_0) + \kappa_l \tag{6}$$

All of the dielectric spectra measured in our study were well represented by eq 5 with the best fit, the five dielectric parameters (ε_l, ε_h, κ_h, κ_l, f_0) were thus obtained, and the dielectric parameters for the systems composed of the NF90 membrane and $MgCl_2$ solution are listed in Table 1. $\Delta\varepsilon$ ($= \varepsilon_l - \varepsilon_h$) in Table 1 is the relaxation increment of permittivity, while $\Delta\kappa$ ($= \kappa_h - \kappa_l$) is the conductivity increment. From Table 1 it is obvious that the relaxation times τ decreased with increasing concentration of $MgCl_2$ aqueous solution; the reason for this phenomenon and the concentration dependency of $\Delta\varepsilon$ and $\Delta\kappa$ will be interpreted in detail in the next section, section 3.2.2. On the other hand, when the concentration of the electrolyte is above 0.1 mol·m^{-3}, the value of β departs from 1 but is still close to 1; this shows that there is a dominant relaxation process in the complex low-frequency relaxation.

3.2.2. Determination of the Low-Frequency Relaxation Mechanism. In order to detect thoroughly which mechanism dominates here, the relaxation increment $\Delta\varepsilon$ and the characteristic frequency f_0 of the low-frequency relaxation are plotted as a function of the concentration c of electrolyte solutions in Figure 4. It can be seen from this figure that both $\Delta\varepsilon$ and f_0 increase proportionally with the electrolyte concentration, which is different from the feature of relaxation in high frequency rising from interfacial polarization.

It is well known that the relaxation time (τ) is the most effective criterion to determine the dielectric relaxation mechanism of different types. Here, for convenient understanding, we introduce the well-known Einstein equation to our analysis

$$\tau = \langle x \rangle^2 / 2D \tag{7}$$

where $\langle x \rangle$ and D are the average displacement and average diffusion coefficient of ions, respectively. According to the literature,[22,23] we supposed that the low-frequency relaxation is due to the counterion polarization in the pores of the membrane; thus, the relaxation time of low-frequency relaxation corresponds to the time for the counterions transporting in the pores from one side of the pore to the other side under the applied electric field E. In this case, the counterions migrate in the cylinder pores, which is characterized by a and b (a and b represent the length and radius of the pore, respectively), as shown in Figure 5.

From Table 1 it can be seen that the value of the low-frequency relaxation time is around 10^{-3} s. Moreover, the diffusion coefficient of Mg^{2+} $D_{(Mg^{2+})} = 7.06 \times 10^{-8}$ m^2·s^{-1}. Therefore, the average displacement of Mg^{2+} can be calculated from eq 7, and its order is 10^{-6}, which is in good agreement with the order of the thickness of the active layer (micrometers). Accordingly, we conclude that the low-frequency relaxations observed in this study are caused by the counterion polarization in the pores of the membrane. This proposition will be described in detail below.

In the presence of an external ac field, as shown in Figure 5, when the frequency is relatively low, the counterions near the pore wall can migrate with the applied ac field, so the time for counterions to transport from one side of the pore to the other is sufficient and then accumulate there (considering that the pores act like a parallel capacitor). As a result, the permittivity of the whole system will increase because of the accumulated charges based on Maxwell's interfacial polarization concept.

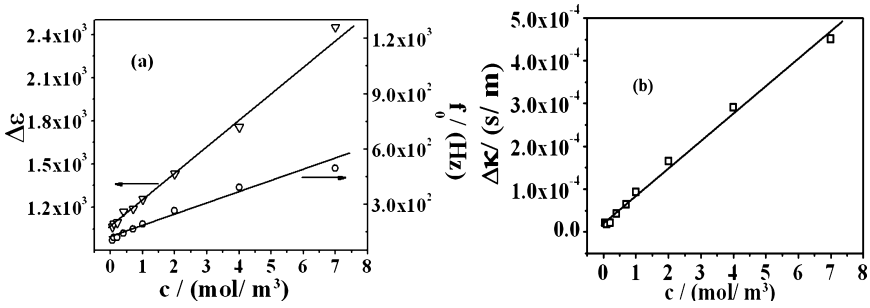

Figure 4. Dielectric relaxation parameters of low-frequency relaxation for the NF90 membrane in $MgCl_2$ electrolyte solutions are plotted against electrolyte concentration: (a) relaxation increment of permittivity $\Delta\varepsilon$ and the character frequency f_0 and (b) relaxation increment of permittivity $\Delta\kappa$.

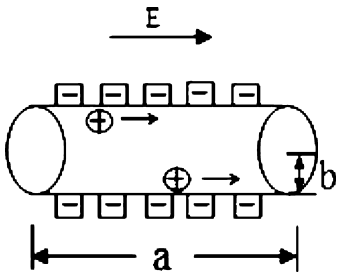

Figure 5. Schematic of the movement of counterions in the pore, where a is the pore's radius, b is the pore's length, and E is the applied electric field.

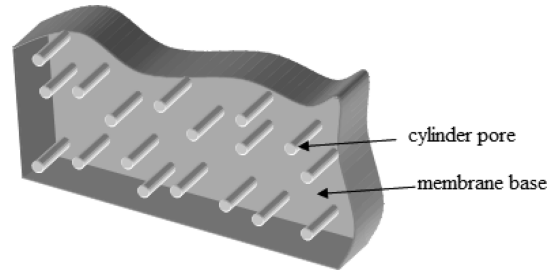

Figure 6. Dielectric model of the active layer of NF membrane with cylinder pores filled with electrolyte solution. The volume fraction of the pores in the membrane base is known as the porosity of the membrane.

On the other hand, when the frequency is higher than the relaxation frequency f_0 (refer to Figure 3), the counterions on the surface the pore wall can no longer migrate with the applied ac field. They will just keep oscillating for a very short distance but cannot reach and accumulate on either side of the pore. For this reason, dielectric relaxation occurs, accompanied with diminishing permittivity due to the decrease of accumulated charge, and increasing conductivity due to the additional oscillation of the counterions. Therefore, the relaxation time of the low-frequency relaxation f_0 can be considered to be equivalent to the time for counterions to migrate from one side of the pore to the other.

3.2.3. Dependence of Dielectric Parameters on Electrolyte Concentrations. To fully understand the low-frequency relaxation, the discussion will be focused on the dependences of dielectric parameters on electrolyte concentrations. From Figure 4 it is obvious that the relaxation frequency f_0 increased with the increment of $MgCl_2$ concentration; this can be considered to be due to the effect of the EDL (electric double layer) on the surface of the pore wall. The electrical properties of the surface can be described by the following equation[30]

$$\lambda^{-1} = \sqrt{\frac{\varepsilon_0 \varepsilon_c kT}{2e^2 C_\infty}} \tag{8}$$

where λ^{-1} is the Debye length or the double-layer thickness on the pore wall, e is the elementary charge, k is the Boltzmann constant, T is the absolute temperature, C_∞ is the number concentration of counterions or coions in the bulk solution, and ε_c is the permittivity of the continuous medium. Here it should be pointed out that in our model, which will be described in the next section, ε_c denotes the permittivity of the membrane base material (i.e., the active layer). Equation 8 shows that the ionic number concentration of electrolyte solution C_∞ is in inverse relation to the thickness of EDL λ^{-1}, that is, the smaller the ionic concentration becomes, the thicker the EDL is. When C_∞ is weak enough, the EDL on the surface of the pore wall leads to an overlapping of the diffuse layers, the EDL will have a greater impact on the transporting of the counterions in the pores[31] and the counterions will need more time to migrate from one side of the pore to the other side. As a result, the relaxation frequency increases with increasing concentration of the electrolyte solution.

To understand the dielectric behavior caused by the pore in depth, we plotted the conductivity increment $\Delta\kappa$ of the low-frequency relaxation against the concentration c of $MgCl_2$ electrolyte solutions, as seen in Figure 4b. From Figure 4a and 4b it is obvious that both $\Delta\varepsilon$ and $\Delta\kappa$ increase monotonously with increasing concentration of the solution. The increase of $\Delta\varepsilon$ is ascribed to the increase of the concentration gradient of electrolyte solution occurring near the surface of the pore wall, whereas the increase of $\Delta\kappa$ can be considered to be due to the ion migration in EDL on the surface of the pore wall. Here, it should be pointed out that the dependence of the relaxation parameters f_0, $\Delta\varepsilon$, and $\Delta\kappa$ on electrolyte concentration c for the other systems composed of different kinds of electrolytes and the three types of NF membranes, which were studied in this paper, are similar with this system, NF90 membrane in $MgCl_2$ electrolyte solution, as shown Figure 4.

3.3. Dielectric Model of Porous Membrane and Improvement of the Expression. According to the discussion in sections 3.2.2 and 3.2.3, the low-frequency relaxation for the system composed of NF membrane and electrolyte solution is confirmed to be caused by the counterion polarization in the pores of the membrane. To obtain more information, such as the structural parameters of the pores and the electrical parameters in the pores, we consider the dielectric model described below: cylinder pores filled with electrolyte solution, acting as the dispersed phase, are dispersing in the continuous phase (here referring to the membrane base material). Therefore, such system is considered to be a disperse system composed of solid membrane and cylinder liquid dispersing in the solid membrane, as shown in Figure 6.

Takashima deduced an expression for the relaxation increment to describe DNA molecules, which can be approximated as a cylinder[24]

$$\varepsilon^* = \frac{e^2 \sigma_0 a^2}{bkT} \frac{9\pi p}{2(1+p)^2} \frac{1}{1 + j\omega\tau} \text{ if } a \gg b \tag{9}$$

where ε^* is the complex permittivity of the "disperse system" in the model, σ_0 is surface density of charged groups on the pore wall, and p is volume fraction of the cylinder pore in the membrane base, which is also referred to as the porosity of the membrane; the other symbols in eq 9 have the same meaning as explained above. Equation 9 could be used to describe the model of the low-frequency relaxation which was generated from the ion transporting in the pore of the membrane, and this model has nothing to do with the bulk electrolyte solution. However, it can be seen from Table 1 that the distribution coefficient of the relaxation time β is below 1; in addition, the electrode polarization may also have little affect on the system; both of them would influence the forming of the low-frequency relaxation. Therefore, eq 5 is no longer suitable for the measured system. To quantitatively calculate the structural and electrical parameters based on the model proposed above, we improved the expression below: the distribution coefficient of the relaxation time β and the electrode polarization term ε_{EP} were

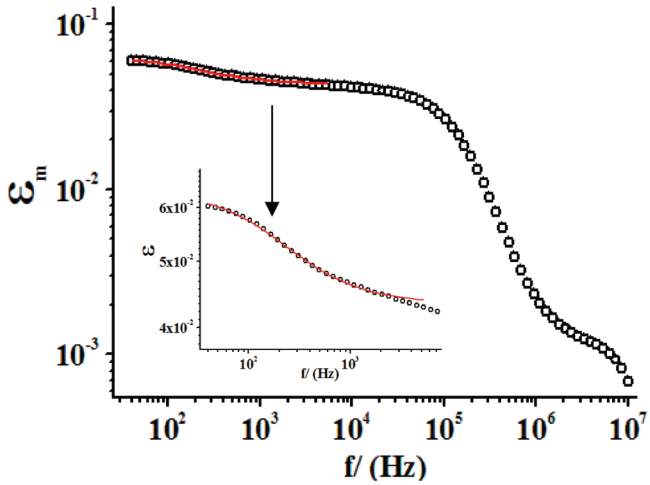

Figure 7. Frequency dependence of membrane permittivity of the system composed of NF90 membrane and 1.0 mol·m^{-3} $MgCl_2$ aqueous solutions: (○) measured results and (—) calculated from the equation 10. The thickness of the membrane used to calculate the permittivity ε_m from its capacitance was 0.2 μm, which was provided by the manufacturer.

introduced to the expression, where ε_{EP} ($= A\omega^{-m}$) is the equivalent permittivity arising from electrode polarization but superposed on the real experimental data and A and m are constants determined experimentally.[32,33] The improved expression is shown in eq 10

$$\varepsilon_m(f) = \frac{e^2\sigma_0 a^2}{bkT\varepsilon_0}\frac{9\pi p}{2(1+p)^2}\frac{1+\left(\frac{f}{f_0}\right)^{\beta}\cos\left(\frac{\pi}{2}\beta\right)}{1+2\left(\frac{f}{f_0}\right)^{\beta}\cos\left(\frac{\pi}{2}\beta\right)+\left(\frac{f}{f_0}\right)^{2\beta}} + A\omega^{-m} + \varepsilon_h \quad (10)$$

It should be noted that eq 10 is the expression of the complex relative permittivity of the membrane.

3.4. Results and Comments. The structural and electrical parameters were obtained by fitting the measured dielectric data with the improved equation (eq 10). These parameters, including the radius b, the length a of the pore, and the surface density σ_0 of charged groups on the pore wall, are used as adjustable parameters to make the calculated dielectric relaxation fit the measured data. In this way, a, b, and σ_0 can be obtained with the best-fitting curves.

Figure 7 shows a typical fitting result for the system composed of NF90 membrane and 1.0 mol·m^{-3} $MgCl_2$ aqueous solutions. From Figure 7 it can be seen that the fitting curve indicated by the solid line is coincides with the measured data in the low-frequency range. The acquired parameters of the system of NF90 membrane in $MgCl_2$ aqueous solutions of various concentrations are listed in Table 2. It is obvious from Table 2 that the radius b and length a of the pore are constant for a type of membrane in electrolyte solution of various concentration. The surface density σ_0 of charged groups on the pore wall increases with increasing concentration of the bulk solution; it can be interpreted in this way: when the concentration of the bulk solution increases, more and more ions will migrate into the pores and σ_0 thus shows a tendency of increasing.

A summary of the average values of various concentrations for a and b of the membrane/electrolyte systems are listed in Table 3. From Table 3 it can be seen that the values of the pore radius b of the three membranes are quite close to that reported in the literature,[34] and the values of the pore length a, which is equal to the thickness of the active layer, are in substantial agreement with the data provided by the manufacturer. These results confirm that the model established in section 3.3 is conformable and reasonable for analyzing the low-frequency relaxation of the nanofiltration membrane.

TABLE 2: Fitting Results for the System Composed of NF90 Membrane and $MgCl_2$ Aqueous Solutions of Various Concentrations by Eq 10

concentration (mol·m^{-3})	σ_0 (10^{11} C·m^{-2})	b (nm)	a (μm)
0.05	1.576	0.2808	0.2337
0.1	2.016	0.2808	0.2337
0.2	4.834	0.2808	0.2337
0.4	7.004	0.2808	0.2337
0.7	9.304	0.2808	0.2337
1.0	10.16	0.2808	0.2337
2.0	12.18	0.2808	0.2337
4.0	13.96	0.2808	0.2337
7.0	13.86	0.2808	0.2337

TABLE 3: Average Values of Various Concentrations for a and b of the System Composed of NF90, NF-, NF270, and the Eight Kinds of Electrolyte Solutions

	NF90		NF-		NF270	
	a (μm)	b (nm)	a (μm)	b (nm)	a (μm)	b (nm)
NaCl	0.2342	0.2832	0.2326	0.3290	0.2329	0.3581
KCl	0.2316	0.2806	0.2337	0.3212	0.2332	0.3551
$MgCl_2$	0.2337	0.2808	0.2315	0.3257	0.2374	0.3410
$CuCl_2$	0.2361	0.2857	0.2334	0.3261	0.2310	0.3609
Na_2SO_4	0.2302	0.2862	0.2362	0.3252	0.2365	0.3631
K_2SO_4	0.2335	0.2814	0.2358	0.3246	0.2338	0.3618
$MgSO_4$	0.2330	0.2873	0.2337	0.3220	0.2319	0.3665
$CuSO_4$	0.2359	0.2851	0.2325	0.3262	0.2383	0.3618
average	0.2335	0.2838	0.2337	0.3250	0.2344	0.3582

The concentration dependence of σ_0 for all systems is shown in Figure 8. It appears in Figure 8 that σ_0 increases sharply at low concentrations with increasing electrolyte concentration and tends to be stable at high concentrations. According to the Donnan equilibrium principle, this phenomenon can be explained by the particular distribution of ions in solution and in membrane with fixed charges. When the concentration of the electrolyte solution is relatively lower, fixed charges in the membrane will strongly attract the counterions into the pores not only to keep them electrically neutral in the membrane but also because the electrochemical potential of ions in the two phases must be equal. In this situation, the concentration of ions in pores increases greatly with σ_0 increasing accordingly. However, when the concentration of the electrolyte solution becomes higher, fixed charges in the membrane are shielded by a large number of counterions and Donnan exclusion partially loses effectiveness, resulting in the increases of σ_0 and an outcome tending to be stable.

It also can be seen from Figure 8 that the difference of increasing rate for the three types of nanofiltration membrane with bulk solution concentration are different in different types of electrolyte solution. In the case of 1:1-type electrolyte, which are shown in Figure 8a and 8b, the order of increasing rate of σ_0 for the three membranes is as follows: NF270 ≈ NF → NF90. The reason for this sequence may be due to the size of the pore's radius, that is, the larger the pore, the easier the counterions migrate into the pore; it is obvious from Table 3 that the pore's radius for NF270 and NF- membranes is larger than that of the NF90 membrane. In the case of the other electrolytes shown in Figure 8c−h,

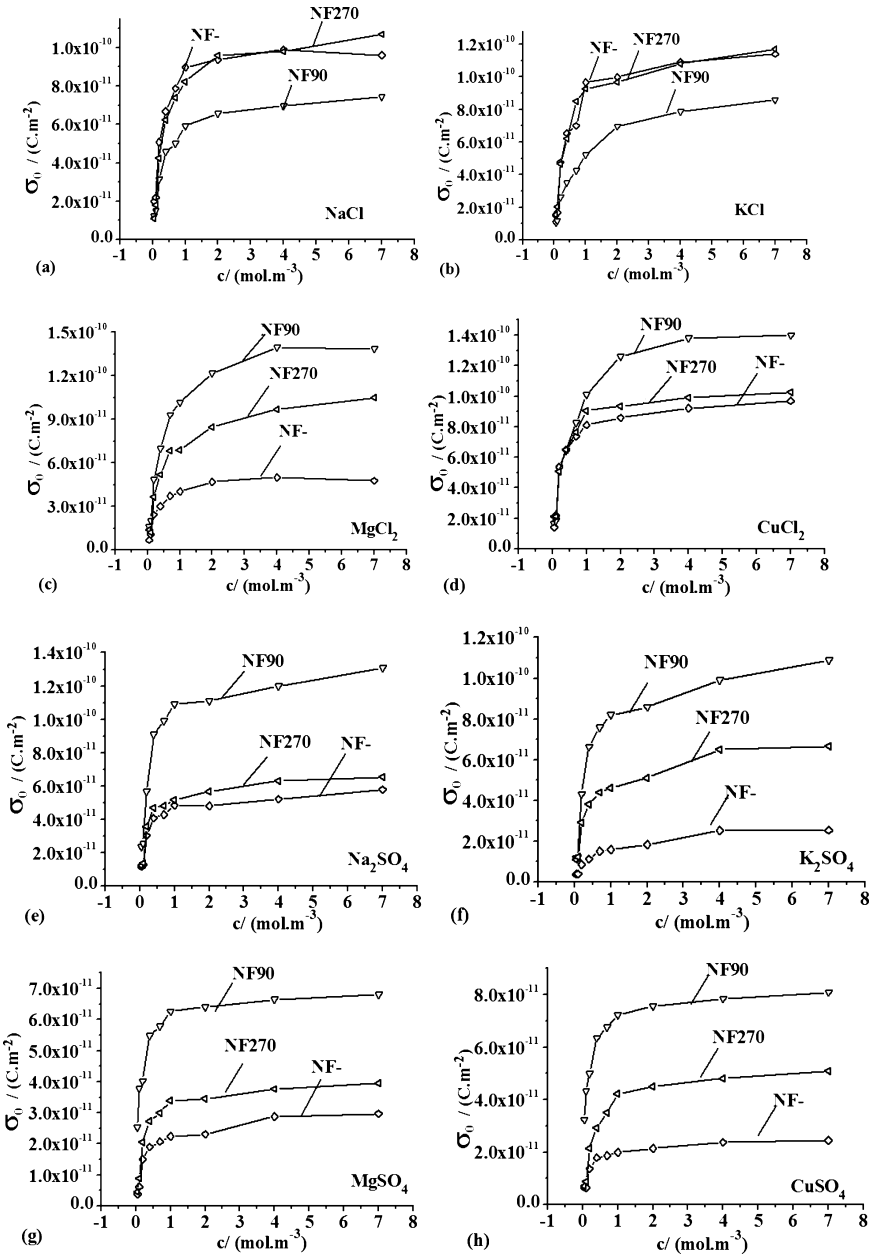

Figure 8. Concentration dependence of σ_0 of NF90, NF-, and NF270 in the eight kinds of electrolyte solutions.

it can be seen that the increasing rate for NF90 is higher than the other two membranes; this is caused by many factors such as the valence of coions and counterions and the Donnan exclusion and dielectric exclusion therefrom.

Another essential parameter related to the pores in the membrane, the zeta potential ζ on the pore−wall, is associated with the surface charged density σ_0 by the Gouy−Chapman expression with regard to the theory of the electric double layer[35]

$$\sigma_0 = -(sign\zeta)\sqrt{(2\varepsilon_0\varepsilon_p RT)\sum_i c_i\left[\exp\left(-\frac{z_i F\zeta}{RT}\right) - 1\right]} \tag{11}$$

where z_i is the valence of ion i, c_i is the concentration of ion i in the pore, which were computed according the literature,[19] and the permittivity of the pore ε_p can be calculated from the following equation based on the obtained parameters above[36]

$$\varepsilon_p = 80 - 2(\varepsilon_w - \varepsilon_d)\left(\frac{d}{b}\right) + (\varepsilon_w - \varepsilon_d)\left(\frac{d}{b}\right)^2 \tag{12}$$

This equation implies that the pore consists of one layer of oriented water molecules with the permittivity ε_d at the pore wall and d is the thickness of the oriented water molecules, according to the literature:[36] ε_d and d are 6 and 0.28 nm, respectively. Because the inside of the pore has the dielectric properties of bulk solution, the value of permittivity in the inside of the pore was taken to be 80 (equal to the permittivity of bulk solution). On the basis of eqs 11 and 12, the zeta potential ζ for all the systems treated with in this work were calculated under the condition of varying the concentration of electrolyte solutions. Figure 9 shows the dependence of the zeta potential ζ on solution concentrations c for systems

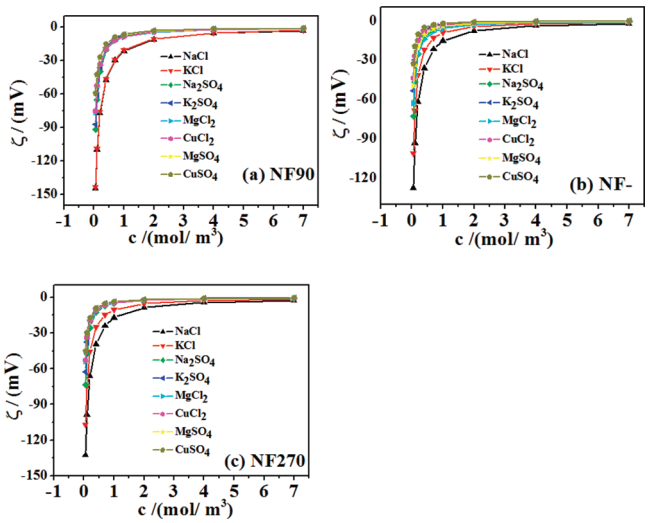

Figure 9. Dependence of the zeta potential ζ on solution concentration c for systems composed of NF membranes and eight kinds of electrolytes: (a) NF90, (b) NF-, and (c) NF270.

composed of NF membranes and eight kinds of electrolytes. It is clearly seen in Figure 9 that the absolute value of the zeta potential ζ decreases sharply with increasing salt concentration at concentrations below 1 mol· m^{-3} and tend to be almost 0 mV at concentrations above 4 mol·m^{-3}; this corresponds to the tendency of the surface charged density σ_0 on the pore wall with the solution concentration c, which was explained by the Donnan equilibrium principle (refer to Figure 8). From Figure 9 it also appears that for any certain membrane of the three types of NF membranes, the value of ζ depends on the type of electrolyte solution in which the membrane was immersed. The most evident case is the one for 1:1-type electrolyte. The absolute value of ζ for all three types of membranes immersed in 1:1-type electrolyte are higher than that in the other types of electrolytes before being a steady value (see Figure 9), indicating that when membranes were immersed in 1:1-type electrolyte, the surface charged density on the pore wall is higher compared to that in the other electrolytes, that is, the three types of studied NF membrane have the lowest retention rate of the 1:1-type electrolyte among the measured electrolytes.

4. Conclusion

Dielectric measurements for the systems composed of three types of NF membranes and eight kinds of electrolyte solutions were carried out over a frequency range from 40 Hz to 11 MHz, and a double-relaxation phenomenon was observed. The main analysis of the present work for the dielectric spectra focused on the low-frequency relaxation, because the relaxation behavior at low frequency shows specificity compared with the ordinary systems reported in most of the literature and the mechanism of the low frequency occurring on membrane systems is controversial. In this article, the mechanism of the low-frequency relaxation was confirmed by fitting dielectric data with the Cole−Cole function; it is closely interrelated to the special structure inside the membrane and was proved to be due to the counterions polarization effect in the pores. In order to interpret this low frequency in detail and obtain the information inside the membrane, we developed a pore membrane based model for analyzing the measured data of the low-frequency relaxation. By using the parameters obtained through analyzing the dielectric data at low frequency, we also successfully calculated the structural parameters of the pore and electrical parameters in the pore, such as the radius and length of the pore, the surface charged density on the pore wall through amended expression for describing the dielectric behavior of a cylinder particle suspension. The values of pore's radius b and pore's length a, which is equal to the thickness of the active layer, are quite close to that reported in the literature. The surface charged density σ_0 on the pore wall increases with increasing concentration of the electrolyte solution, and the tendency was explained by the Donnan equilibrium principle. Meanwhile, the calculated results show that the order of the increasing rate of σ_0 for NF90, NF-, and NF270 is different in different types of electrolytes. This is a result brought by many facts such as the pores' radius, the porosity of the active layer, the fixed charge of the active layer, and the Donnan exclusion and dielectric exclusion accompanied with the fixed charge of the active layer. Additionally, the zeta potential ζ on the pore wall as a function of electrolyte concentration in bulk solution was obtained based on the surface charge density σ_0; the absolute value of ζ decreases with increasing salt concentration and tends to be almost 0 mV at concentrations above 4 mol·m^{-3}. For all three types of NF membranes, the absolute value of the zeta potential ζ on the pore wall of the 1:1 electrolytes is the lowest compared with the others types of electrolytes, which indicates that the studied NF membrane has a lower retention rate of the 1:1-type electrolyte versus the other types of electrolytes. In summary, the values of the structural parameters of the pore in NF membrane and electrokinetic parameters inside the pore of the membrane under varying electrolyte species and concentrations for three types of NF membrane were obtained only by dielectric measurements and analyzing without any other tests and means.

This research developed a new skill to probe inner information of multilayer membrane systems in a noninvasive way and shows that dielectric spectroscopy is an effective method to get detailed electrical and structural parameters about the inner structure of the separation membrane. Moreover, this study may provide a new idea for treating with other heterogeneous systems such as a microporous particle suspension.

Acknowledgment. This work was financially supported by the National Nature Science Foundation of China (Nos. 20673014 and 20976015).

References and Notes

(1) Raman, L. P.; Cheryan, M.; Rajagopalan, N. *Chem. Eng. Prog.* **1994**, *90*, 68.
(2) Childress, A. E.; Elimelech, M. *Environ. Sci. Technol.* **2000**, *34*, 3710.
(3) Schaep, J.; Vandecasteele, C. *J. Membr. Sci.* **2001**, *188*, 129.
(4) Lanteri, Y.; Szymczyk, A.; Fievet, P. *J. Phys. Chem. B.* **2009**, *113*, 9197.
(5) Sbaï, M.; Szymczyk, A.; Fievet, P.; Sorin, A.; Vidonne, A.; Pellet-Rostaing, S.; Favre-Reguillon, A.; Lemaire, M. *Langmuir* **2003**, *19* (21), 8867.
(6) Xu, T. W.; Hu, K. Y. *Sep. Purif. Technol.* **2004**, *40*, 231.
(7) Shang, W. J.; Wang, X. L.; Yu., Y. X. *J. Membr. Sci.* **2006**, *285*, 362.
(8) Asami, K. *Prog. Polym. Sci.* **2002**, *27*, 1617.
(9) Zha, F. F.; Coster, H. G. L.; Fane, A. G. *J. Membr. Sci.* **1994**, *93*, 255.
(10) Coster, H. G. L.; Kim, K. J.; Dahlan, K.; Smith, J. R.; Fell, C. J. D. *J. Membr. Sci.* **1992**, *66*, 19.
(11) Kavanagh, J. M.; Hussain, S.; Chilcott, T. C.; Coster, H. G. L. *Desalination* **2009**, *236*, 187.
(12) Fortunato, R.; Branco, L. C.; Afonso, C. A. M.; Benavente, J.; Crespo, J. G. *J. Membr. Sci.* **2006**, *270*, 42.
(13) Zholkovskij, E. K. *J. Colloid Interface Sci.* **1995**, *169*, 267.
(14) Park, J.-S.; Choi, J.-H.; Woo, J.-J.; Moon, S.-H. *J. Colloid Interface Sci.* **2006**, *300*, 655.

(15) Naumowicz, M.; Petelska, A. D.; Figaszewski, Z. A. *Electrochim. Acta* **2005**, *50*, 2155.
(16) Kelly, M. J.; Egger, B.; Fafilek, G.; Besenhard, J. O.; Kronberger, H.; Nauer, G. E. *Solid State Ionics* **2005**, *176*, 2111.
(17) Li, Y. H.; Zhao, K. S.; Han, Y. *Sci. China, Ser. B: Chem.* **2008**, *51*, 813.
(18) Zhao, K. S.; Li, Y. H. *J. Phys. Chem. B* **2006**, *110* (6), 2755.
(19) Li, Y. H.; Zhao, K. S. *J. Colloid Interface Sci.* **2004**, *276*, 6876.
(20) Foster, K. R.; Schwan, H. P. *CRC Crit. Rev. Biomed. Eng.* **1989**, *17* (1), 25.
(21) Shilov, V. N.; Delgado, A. V.; González-Caballero, F.; Horno, J.; López-García, J. J.; Grosse, C. *J. Colloid Interface Sci.* **2000**, *232*, 141.
(22) Kuang, W.; Nelson, S. O. *J. Colloid Interface Sci.* **1997**, *193*, 242.
(23) Martinsen, Ø. G.; Grimnes, S.; Karlsen, J. *J. Colloid Interface Sci.* **1998**, *199*, 107.
(24) Takashima, S. *Electrical Properties of Biopolymers and Membranes*; Adam Hilger: Philadelphia, 1989.
(25) Asaka, K. *J. Membr. Sci.* **1990**, *50*, 71.
(26) Asami, K.; Irimajiri, A.; Hanai, T.; Koizumi, N. *Chem. Res., Kyoto Univ.* **1973**, *51*, 231.
(27) Hanai, T. *Emulsion Science*; Sherman, P., Ed.; Academic: New York, 1968.
(28) Ashcroft, R. G.; Coster, H. G. L.; Smith, J. R. *Biochim. Biophys. Acta* **1977**, *469*, 13.
(29) Hanai, T.; Imakita, T.; Koizumi, N. *Colloid Polym. Sci.* **1982**, *260*, 1029.
(30) Adamson, A. W. Gast, A. P. *Physical Chemistry of surfaces*, 6th ed.; Wiley: New York, 1997.
(31) Friedmann, H.; Amiri, O.; Aït-Mokhtar, A. *Cem. Concr. Res.* **2008**, *38*, 1394.
(32) Schwan, H. P. *Physical techniques in biological research*; Academic: New York, 1963.
(33) Zhao, K.-S.; Chen, Z. *Colloid Polym. Sci.* **2006**, *84*, 1147.
(34) Hilal, N.; Al-Zoubi, H.; Darwish, N. A.; Mohammad, A. W. *Desalination* **2005**, *177*, 187.
(35) Szymczyk, A.; Fatin-Rouge, N.; Fievet, P.; Ramseyer, C.; Vidonne, A. *J. Membr. Sci.* **2007**, *287*, 102.
(36) Mohammad, A. W.; Hilal, N.; Al-Zoubi, H.; Darwish, N. A. *J. Membr. Sci.* **2007**, *289*, 40.

JP110160Z